Liquid Crystals
Publication details, including instructions for authors and subscription information:
http://www.informaworld.com/smpp/title~content=t713926090

Director orientation in chevron surface-stabilized ferroelectric liquid crystal cells. Verification of orientational binding at the chevron interface using visible polarized light transmission spectroscopy

J. E. Maclennan[a]; N. A. Clark[bc]; M. A. Handschy[d]; M. R. Meadows[d]
[a] Institute of Physical Chemistry, University of Mainz, Mainz, F. R. Germany [b] Condensed Matter Laboratory, Department of Physics, and Center for Optoelectronic Computing Systems, University of Colorado, Boulder, Colorado, U.S.A. [c] Department of Physics, University of Colorado, Boulder, Colorado, U.S.A. [d] Displaytech, Inc., Boulder, Colorado, U.S.A.

To cite this Article Maclennan, J. E. , Clark, N. A. , Handschy, M. A. and Meadows, M. R.(1990) 'Director orientation in chevron surface-stabilized ferroelectric liquid crystal cells. Verification of orientational binding at the chevron interface using visible polarized light transmission spectroscopy', Liquid Crystals, 7: 6, 753 — 785
To link to this Article: DOI: 10.1080/02678299008033839
URL: http://dx.doi.org/10.1080/02678299008033839

LIQUID CRYSTALS, 1990, VOL. 7, NO. 6, 753–785

Director orientation in chevron surface-stabilized ferroelectric liquid crystal cells

Verification of orientational binding at the chevron interface using visible polarized light transmission spectroscopy

by J. E. MACLENNAN†, N. A. CLARK‡§, M. A. HANDSCHY¶ and M. R. MEADOWS¶

‡ Condensed Matter Laboratory, Department of Physics, and Center for Optoelectronic Computing Systems, University of Colorado, Boulder, Colorado 80309-0390, U.S.A.

¶ Displaytech, Inc., 2200 Central Avenue, Boulder, Colorado 80301, U.S.A.,

† Institute of Physical Chemistry, University of Mainz, Mainz, F.R. Germany

(*Received 21 May 1989; accepted 10 December 1989*)

We present results of theoretical modelling and experimental study of director distributions and the associated optical properties of chevron surface stabilized ferroelectric liquid crystal (SSFLC) cells. Chevron cells are modelled as being two stacked FLC slabs, described by distinct orientation distributions of the director $\hat{n}$-polarization $\mathbf{P}(\hat{n} - \mathbf{P})$ couple. In each slab the $\hat{n} - \mathbf{P}$ distribution is governed by bulk Frank elastic and electric field-induced torques and by surface torques at the FLC-solid interface and at the chevron interface, where the two distributions are coupled. The optical properties of such structures are calculated numerically and the results tested using polarized light microscope-based spectrophotometric measurements of the wavelength dependent transmission of chevron SSFLC cells with varying sample orientation and applied field. Measured transmission spectra agree quantitatively with the model and provide evidence for the constraint of the $\hat{n} - \mathbf{P}$ field at the chevron interface, particularly in the case when the chevron interface is displaced from the cell midplane.

1. Introduction

The unique properties of ferroelectric liquid crystals (FLCs) can be exploited to make a variety of useful electro-optic devices. Cells in the surface-stablized (SSFLC) geometry are particularly interesting since they exhibit multiple stable states and can be driven rapidly between them with applied electric fields. The simplest SSFLC geometry, described by Clark and Lagerwall [1], has the smectic layers oriented uniformly, approximately normal to the bounding plates (the 'book-shelf' geometry). These cells have two possible uniform director states, either of which can cause extinction when the cell is correctly oriented between crossed polarizers. One finds these and many other SSFLC cells, however, which clearly have *non-uniform* director structures, as evidenced by the fact that they cannot be made to extinguish at any orientation between crossed polarizers, merely changing their birefrinence colour as they are rotated. The recent discovery of chevron layer structure

§ Address for reprints: Department of Physics, University of Colorado, CB 390, Boulder, Colorado 80309, U.S.A.

0267-8292/90 $3.00

by Rieker *et al.* [2, 3] has improved our understanding of the appearance and behaviour of a large class of such non-uniform cells in applied electric fields. In this paper we present a detailed model of the director structure in chevron cells and use it to predict their electro-optical properties.

2. Theory

2.1. *Surface-stablized director structures*

We begin by briefly reviewing the earlier work upon which our current model is based. The first theoretical models of SSFLC cells were developed by Handschy, Clark and Lagerwall [4, 5], who argued that the director orientation structures and field induced transitions found in these cells were the combined result of the usual elastic coupling between LC molecules and the presence of significant and unusual interactions with the bounding surfaces. Ferroelectric liquid crystals, like nematics, experience a non-polar interaction with the bounding plates that constrains the directors to be either perpendicular or parallel to the plates, giving what is referred to as 'homeotropic' or 'planar' alignment respectively. The chiral nature of FLC molecules allows, in addition, a novel polar interaction with the glass that favors a specific direction of the polarization at the bounding surfaces, i.e. either towards or away from the plates. Mathematical models of these surface energies will be presented later. In an idealized bookshelf geometry with the smectic layers normal to the plates, as illustrated in figure 1, both of these surface interactions preferentially orient the molecules parallel to the plates. The non-polar term alone stabilizes two surface states which are characterized by the polarization orientations $\phi = 0$ and $\phi = \pi$, where ϕ is the angle between **P** and the x axis, and which have directors oriented at opposite extremes of the FLC tilt cone [1]. The effect of the polar interaction is to favour one of these orientations over the other. If the plates are similarly prepared and the polar interaction is strong enough [4], the zero field state will be a splayed one, with the director precessing on the tilt cone from one state to the other between the bottom and the top of the cell, as shown in figure 2 (*a*).

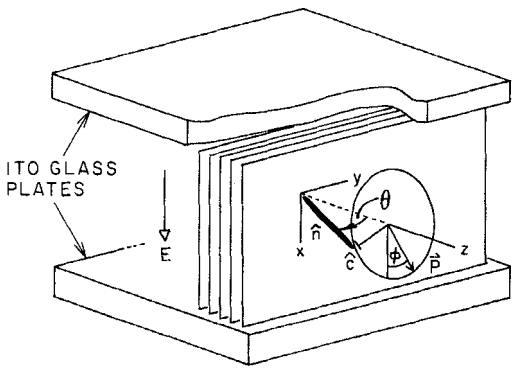

Figure 1. FLC cell with bookshelf geometry. The molecular director $\hat{n}$ is constrained to a tilt cone of angle θ oriented about the smectic layer normal $\hat{z}$. The spontaneous ferroelectric polarization **P** is in the direction $\hat{z} \times \hat{n}$, lying in the smectic layer (x–y) plane and , in the absence of electric field, making an angle ϕ with the x-axis. An applied field **E** exerts a $\mathbf{P} \times \mathbf{E}$ torque which favours $\phi = 0$ and causes the molecules to reorient on the tilt cone so that **P** points more along $\hat{x}$.

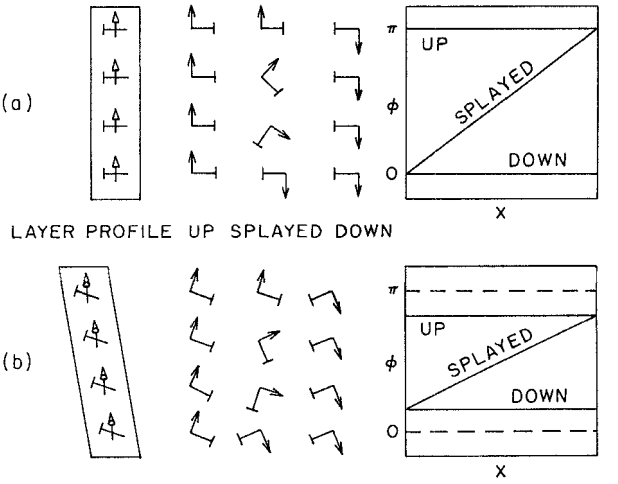

Figure 2. Surface-stablized states in FLC cells. Depending on their relative strength, the polar and non-polar FLC-surface interactions can stabilize either uniform or splayed states at zero field. This is illustrated in two cases: (*a*) with smectic layers normal to the glass; and (*b*) with tilted layers, which requires a surface pretilt of the polarization in order to maintain planar orientation of the directors. The ferroelectric polarization **P** is represented by '→' and the *c*-director $\hat{c}$, which is the projection of the molecular director $\hat{n}$ onto the smectic layer plane, by '⊣'.

If the layers are tilted, the director can maintain planar orientation by moving on the tilt cone, as illustrated in figure 2 (*b*). When the layers are tilted back, for example, the ferroelectric polarization **P**, which is confined to the layer plane, rotates away from the original equilibrium orientation of $\phi = 0$ or $\phi = \pi$ towards $\phi = \pi/2$. The resulting 'pretilt' of the polarization [4] has been a central concept in explaining many observed switching phenomena in SSFLC cells. In particular, a variety of pretilt conditions enable switching between multiple stable nonuniform states [5], including bistable splayed states [6].

SSFLC cells exhibit a variety of interesting and peculiar textures when viewed in polarized light. One particularly intriguing problem has been to explain the nature of so-called 'zig-zag' defects, the distinctive jagged lines found in many splayed cells that separate splayed regions which have the same average polarization state (UP or DOWN) and show the same general birefringence colour but with different intensity. Handschy and Clark proposed [4] that in cells with zig-zag defects the smectic layers were tilted relative to the glass plates and that the direction of the layer tilt changed across the zig-zag wall but this could not easily be verified purely by optical microscopy. Early on, transmission spectrometry using polarized light seemed to us a reasonable way of probing the director orientation in splayed SSFLC cells but was met initially with only moderate success [7].

These problems also attracted the interest of the group of Fukuda and Takezoe in Tokyo, who made significant progress in understanding cells with zig-zag walls (see, for example, [8, 9], both of which contain further references to other publications of the Tokyo group). Two of their more important findings, in the light of our present discussion, were (1) that the main colour-changing switching process in these cells is mediated by domain walls which are removed from the cell surfaces; and (2) that the colour difference between the UP and DOWN domains at zero field could be

explained qualitatively by assuming that these corresponded to non-uniform director structures with opposite polarization reorientation (clockwise or counterclockwise) as the cell is transversed. In support of the latter conjecture, numerical calculations and chromaticity diagrams were used to show that the perceived colours of these oppositely twisted states were similar to those of real cells [10].

2.2. *Director structure of chevron cells*

It was not until the X-ray experiment of Rieker and Clark finally revealed that zig-zag cells have a chevron-shaped layer structure [2, 3], that we were able to develop a complete model of the director orientation in these cells that agreed with experiment. Basically chevron cells comprise two slabs of FLC material, with layers tilted equally and by opposite amounts from the cell normal, stacked on top of each other. The layers thus form a chevron-shaped structure (> > > > > >), and the direction of the chevrons change across the zig-zag wall [3]. The slabs are joined at a narrow, planar interface (the 'chevron interface') oriented parallel to the bounding plates and along which domain walls move under the influence of applied fields. The chevron interface is not necessarily in the middle of the cell and is reflected through the mid-plane of the cell as a zig-zag defect is crossed. The geometry of the chevron cell is shown in figure 3.

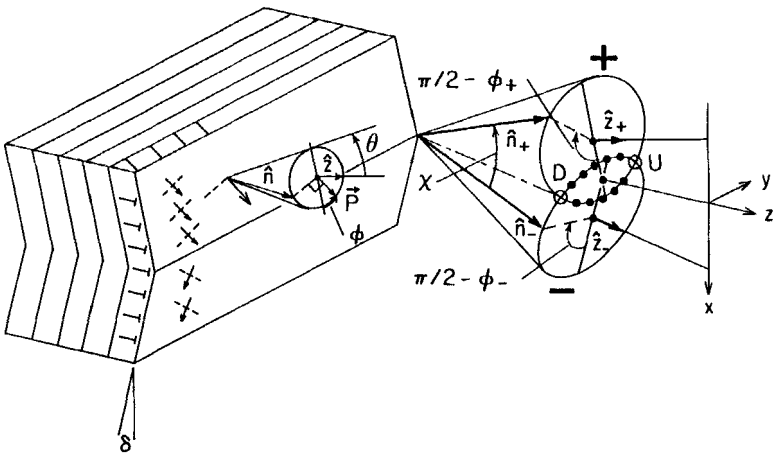

Figure 3. Geometry of the director field at a smectic C chevron : (*a*) The smectic C is a locally biaxial structure of liquid-like layers in which $\hat{n}(\mathbf{r})$ is tilted at an equilibrium angle θ relative to the local layer normal $\hat{\mathbf{z}}_+(\mathbf{r})$ or $\hat{\mathbf{z}}_-(\mathbf{r})$ and is free to reorient azimuthally through the angle ϕ on a cone of axis $\hat{\mathbf{z}}_+$ (or $\hat{\mathbf{z}}_-$). Subscripts + and − refer to quantities on opposite sides of the chevron. For $\delta < \theta$, the cone intersections U and D (open circles) are the equilibrium orientations of $\hat{n}$, having $\hat{n}$ parallel to the interface. In these states the FLC polarization **P** is pretilted such that starting from the D state and applying a field **E** along $\hat{\mathbf{x}}$, the polarizations rotate in opposite directions on opposite sides of the chevron, moving along the dotted paths from D to U for sufficiently large E. Reproduced from [3].

In summary, our model of the director structure in chevron cells assumes that with no applied electric field strong surface interactions locally constrain the molecules to be approximately parallel to the bounding plates. The director orientation varies essentially continuously in the rest of the cell under the influence of the bulk elasticity. Thus we take the polarization density to be small enough that fields due to

polarization space charge are negligible, that is $\sqrt{(K/P^2)} > d$, where K is the effective Frank constant and d is the sample thickness. Applied fields can reorient the molecules and thereby change the effective birefringence. We assume that intermolecular forces try to minimize any discontinuity in the director field across the chevron interface, i.e. there is orientational binding there. Since the smectic layers above and below the chevron interface are oppositely tilted, their SC tilt cones intersect each other in general at only two places. At these positions, the directors are parallel to both the chevron interface and the bounding plates of the cell and can have a (pretilted) polarization either UP or DOWN (see figure 3). The polarization orientation angle ϕ that gives these director orientations obeys the relation

$$\sin\phi = \pm \frac{\tan\delta}{\tan\theta},$$

which for $\theta = 22°$ and a layer tilt of $\delta = 18°$ gives $\phi = \pm 53°$ and $\phi = \pm 127°$.

As in the case of uniformly tilted layering discussed in the previous section, we would expect appropriately treated surfaces to stabilize several possible states, either uniform UP, uniform DOWN, splayed UP or splayed DOWN as shown in figure 4. With identically treated surfaces (which we will assume to be the case) there are, in principle, two possible set of splayed states, one with $\hat{P} \cdot \hat{s} > 0$ and the other with $\hat{P} \cdot \hat{s} < 0$, where $\hat{s}$ is the outward-directed FLC surface normal. Which states occur

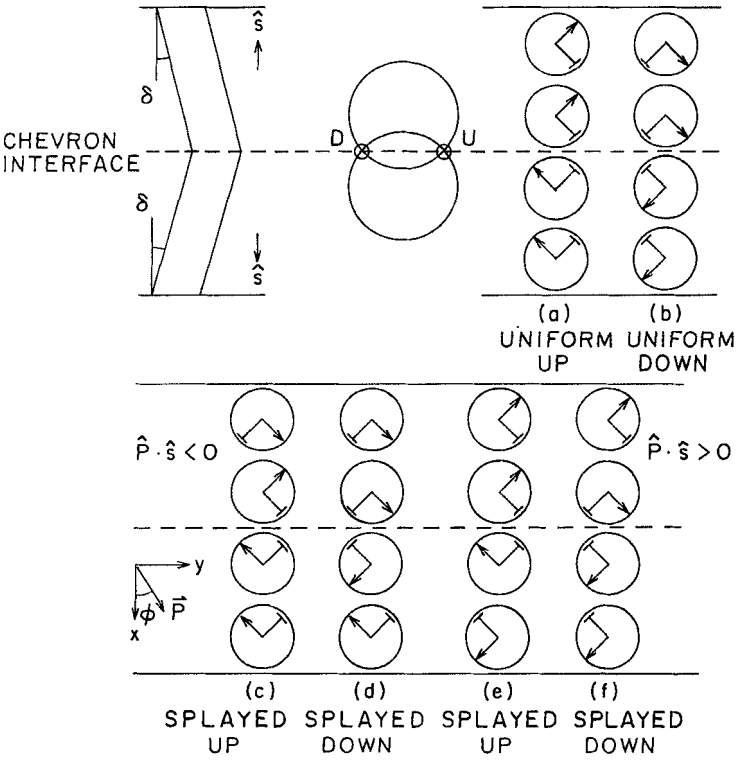

Figure 4. Director states in chevron cells. In FLC cells with chevron layer geometry, planar surface anchoring conditions stabilize several different uniform and splayed states. With identically treated glass bounding plates, we would expect to get one of the two pairs of splayed equilibrium states (i.e. either (*c*) and (*d*) or (*e*) and (*f*)), depending on whether the surfaces prefer $\hat{P} \cdot \hat{s}$ positive or negative.

depends on the surface energy anisotropy and can be distinguished experimentally by optical properties.

In an idealized model cell, the director at every interface is parallel to the glass plates at zero field. We thus implicity assume the presence of a polar interaction energy to stabilize a splayed equilibirum state but for the purpose of illustration ignore the fact that the polar term would also cause a slight reduction of the polarization pretilt at the glass [11, 12]. In a real cell we would not expect to observe our idealized zero-field structures but ones with slightly different surface orientations, as confirmed by Xue *et al.* [13].

Continuity of the director field across the chevron interface leads automatically to a discontinuity in **P**. This favours opposite signs of polarization pretilt at the top and bottom plates, which has as a consequence the important result that the two non-uniform states (which we shall from now on refer to as 'UP' and 'DOWN') must have opposite signs of polarization splay. These states therefore have different average polarization and so different average director orientation, which explains in essence why the UP and DOWN states in chevron cells exhibit such different birefringence colours. An approximate analytical justification of these spectral differences has recently been performed by Hiji and others of the Tokyo group [14] but using simpler splayed states that are distinctly different from ours.

When an electric field is applied to the sample, the directors in both slabs reorient (in opposite senses) on their tilt cones in an effort to align **P** more closely with **E**. Given some boundary angles, the director orientation $\phi(x)$ is found by solving the appropriate field equation independently in each slab. The molecules at the chevron interface reorient in a complicated way, no longer able simply to minimize the director discontinuity across the chevron interface [12]. For simplicity we assume here that the reorientation is symmetric immediately above and below the chevron.

As an example of what happens in a typical cell, consider applying a DOWN field to an UP state, which immediately results in unstable director orientations both at the chevron interface and at the bottom of the cell (see figure 4(*c*)). In practice, the chevron usually switches first (or at lower field) via the motion of domain walls, causing a dramatic colour change. The lower surface is more difficult to reorient and the accompanying colour changes are much more continuous. This latter reorientation is first order [15] and it requires a very high field to switch the cell all DOWN [13].

In the rest of this paper, we will give a mathematical description of the director orientation structure in splayed chevron cells and show how the director orientation can be used to calculate the cell's optical properties. As an example, we will show how a large measure of optical extinction can be obtained in non-uniform chevron cells with appropriately oriented polarizers, even when the Mauguin limit is not obeyed and there is no waveguide-like propagation of polarized light. The calculations also confirm that the difference in intensity between two domains separated by zig-zag defect can be directly attributed to the repositioning of the chevron interface by reflection through the mid-plane of the cell. Finally, we compare measurements of the visible transmission spectrum of a real chevron cell placed between crossed polarizers with the results of numerical model calculations in order to see how the director orientation in the cell changes with applied electric field.

2.3. *Mathematical description of director field*

The general dependence of $\phi(x)$ on applied field is found, in regions far from domain walls, by solving the one-dimensional differential equation for the director

field derived by minimizing the FLC free energy. We consider both bulk and surface energies, in the manner of Handschy and Clark [4], but generalize their expression to account for tilted layers and the presence of the chevron interface. If we assume that the only variation of the director orientation is in the direction normal to the cell walls (i.e. along the x axis) and results from reorientation on the smectic C tilt cone, then the total free energy of a cell of thickness d can be approximated by

$$F = \int_{-d/2}^{d/2} K\phi_x^2 - PE\cos\phi + Kq_s \sin\phi\phi_x dx$$
$$- \gamma_1(\cos^2\psi_b + \cos^2\psi_t) - \gamma_2 \cos\delta(\cos\phi_t - \cos\phi_b) - \gamma_4 \cos\chi. \quad (1)$$

We have assumed an isotropic elasticity with distortions of the c-director characterized by the elastic constant K. This is related to K_n, the Frank elastic constant for distortions of the director field, by $K \approx K_n \sin^2\theta$, where θ is the SC tilt angle; q_s is the wavevector of spontaneous splay characteristic of ferroelectric smectics [15]. **P** is the ferroelectric polarization, which makes an angle ϕ relative to **E**, the electric field applied along the $+\hat{x}$ axis. The γ_i are surface energy anisotropies and the subscripts b and t refer to the bottom and top of the cell respectively. ψ_b and ψ_t are the director elevation angles at the glass plates and χ is the angle (assumed small) between molecular directors immediately on either side of the chevron interface [12]. We have ignored the flexoelectric and dielectric energies [16]. Scaling x by the cell thickness d gives

$$\frac{Fd^2}{K} = \int_{-1/2}^{1/2} \phi_x^2 - \lambda_3^2 \cos\phi\, dx$$
$$- \lambda_1(\cos^2\psi_b + \cos^2\psi_t) - \lambda_2 \cos\delta(\cos\phi_t - \cos\phi_b) - \lambda_4 \cos\chi, \quad (2)$$

where the surface interactions are determined by $\lambda_1 = \gamma_1 d/K$, $\lambda_2 = (q_s + \gamma_2/K)d$, $\lambda_4 = \gamma_4 d/K$. The applied field strength is given by $\lambda_3^2 = (PEd^2/K) = (d/\xi)^2$, and $\xi = (K/PE)^{1/2}$ defines the electric field correlation length. The equilibrium state that minimizes this free energy satisfies simultaneously the Euler–Lagrange equation

$$\phi_{xx} = \lambda_3^2 \sin\phi \quad (3)$$

and a set of surface torque balance equations at each interface that are essentially boundary conditions on the slope [1, 12]. (Tilting the smectic layers means that the effective electric field strength in equation (3) should be reduced to $\lambda_3^2 \cos\delta$ but this is typically a small correction and we have ignored it.)

We briefly sketch the solution of this field equation, which is just the equation of motion of a simple pendulum. In the absence of field, equation (3) reduces to Laplace's equation $\phi_{xx} = 0$, which is solved by $\phi = Ax + B$. This describes the uniform and uniformly splayed states shown in figure 2. In the general case of non-zero field, equation (3) can be integrated once to give

$$\phi_x^2 = 2\lambda_3^2(\cos\phi_0 - \cos\phi),$$

where $\phi_0 \equiv \phi(x :: \phi_x = 0)$ defines the inflection point in the $\phi(x)$ curve. Making the substitutions $\cos\phi = 2k^2 \sin^2\mu - 1$ and $\cos\phi_0 = 2k^2 - 1$ and integrating across the entire sample recasts the problem in the standard form an an elliptic integral

$$\int_{-1/2}^{1/2} \lambda_3 dx = \int_{n_t}^{n_b} \frac{-du}{\sqrt{(1 - k^2 \sin^2 u)}},$$

where the labels t and b stand for 'top' and 'bottom' as before. For the sake of consistency with earlier work [4], the x-axis in our geometry points DOWN, in the direction of a positive E-field (see figure 1). This integral equation can be solved for the parameter k, which corresponds roughly to the amount of curvature of the ϕ vs. x graph. With fixed boundaries, the curvature depends only on the strength of the electric field, through the parameter λ_3. Having determined k, we now integrate to an arbitrary position in the cell, obtaining

$$\int_{-1/2}^{x} \lambda_3 dx = \int_{n_t}^{\eta} \frac{-du}{\sqrt{(1 - k^2 \sin^2 u)}}$$

which can be written as

$$F(\eta, k) = F(\eta_t, k) - \lambda_3(x + 1/2),$$

where we have used the notation of Abrahamowitz and Stegun [17] for incomplete elliptic integral $F(\eta, k)$. This equation is solved in turn using the jacobian elliptic function $\mathrm{sn}(u, k)$ defined by $\mathrm{sn}(F(\eta, k); k) = \sin\eta$ to get

$$\sin\eta = \mathrm{sn}(F(\eta_t, k) - \lambda_3(x + 1/2); k)),$$

which can be solved for η and hence for ϕ as a function of x.

This general technique, with some modifications, is used to solve for a variety of director profiles in model FLC cells, the shapes of which are determined only by the applied field strengths and the chosen boundary conditions. Some typical solutions for both splayed and uniform zero-field states are shown in figure 5, where we have kept the boundaries fixed for simplicity. The physical parameters used there are similar to those used to model the experimental data presented later on. For these moderate voltages the polarization field distorts relatively little from the zero-field state and it is important that the boundary angle also be allowed to change with field in order to achieve the kinds of optical changes observed in real cells.

2.4. *Visible transmission spectroscopy*

We have devised and built a computer-based spectrometer to do spectral analysis of visible light transmitted by FLC cells as a probe of how molecular orientation varies with applied electric field. By comparing calculated spectra with experimental results we can determined the director structure in different SSFLC cells. In addition, this technique is a sensitive probe of director orientation at cell surfaces that should enable us to characterize the LC-surface interaction that is fundamentally responsible for the properties of SSFLC devices.

Our method is based on the well known optical anisotropy (birefringence) of FLCs, which behave essentially as locally optically uniaxial media with the optic axis along the director $\hat{n}$, the local average molecular orientation direction. (The biaxiality of the LC molecules is a small effect and will be ignored in this treatment [18].) The principal effect of applied field is to change $\phi(x)$, the azimuthal orientation of $\hat{n}$ about the layer normal, as shown in figure 5. The tilt angle θ between $\hat{n}$ and $\hat{z}$ can be taken to be fixed. In general ϕ will depend on x, the coordinate normal to the cell bounding plates, and in absence of applied field can either be indpendent of x (uniform state), or can depend on x (splayed state). For SSFLC samples from one to a few microns thick between crossed polarizers, the LC optical anisotropy leads to the appearance of birefringence colours in the transmitted light for incident white light. That is, the

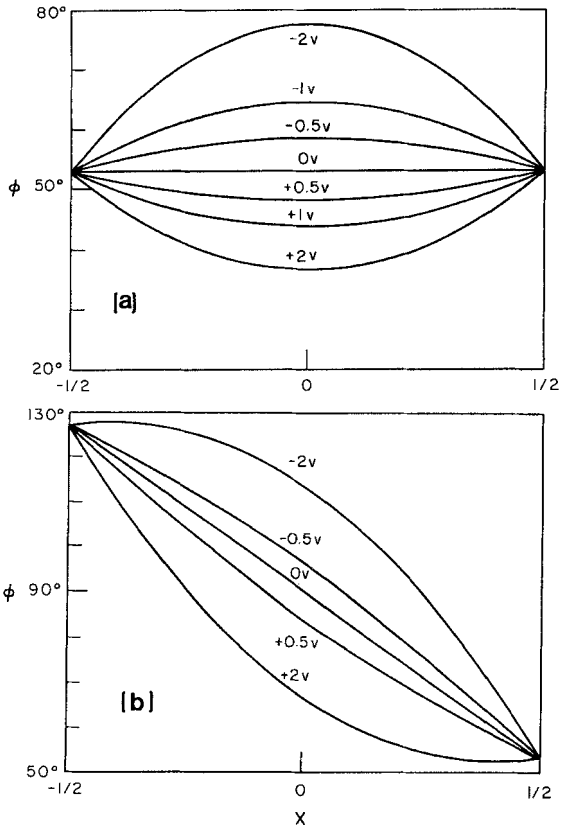

Figure 5. Polarization states as a function of applied electric field. The distorted states are obtained by solving equation (3) at different fields. The zero-field states are (*a*) uniform ($\phi_b = \phi_t = 53°$); and (*b*) splayed ($\phi_b = 127°$, $\phi_t = 53°$). The cell is $d = 3.9\,\mu m$ thick and contains an FLC with $P/K = 1(V\,\mu m)^{-1}$.

cell transmission is a function of the optical wavelength and depends on the cell thickness, refractive index anisotropy of the FLC material and the molecular orientation. If the refractive indices and cell thickness are known, then the transmitted light becomes a probe of the molecular orientation.

If ϕ is independent of x, the molecular orientation can readily be calculated from the birefringence spectrum using the theory of uniform birefringent media. However, the general case of interest for field effects in SSFLC devices has $\phi(x)$ non-uniform and the net effect of the FLC medium on the polarization properties of incident light must be calculated numerically. A brief history of the development of efficient mathematical techniques for calculating light propagation in liquid crystals is given by Ong and Meyer [19]. We have used the '4 × 4 matrix technique' devised originally by Berreman to study light propagation in nematic and chiral nematic phases [20]. This involves dividing the liquid crystal layer into thin strata in which ϕ is uniform and numerically propagating the fields from stratum to stratum by solving Maxwell's equations. This technique is readily applicable to the ferroelectric case where ϕ depends on the single coordinate x [10, 21]. Hence, if the LC refractive indices, smectic tilt angle θ, and layer tilt δ are known, then for a given orientation of polarizer and analyser and orientation distribution $\phi(x)$, the cell transmission spectrum can be calculated.

2.5. *Optical model of FLC structure*

Our optical model for an FLC cell is a slab of locally uniaxial material with the spatially varying optic axis (OA) orientation (i.e. the director) fixed at the boundaries and obeying equation (3) in the bulk. For chevron cells we take two such slabs, stacked one on top of the other. Apart from the layer tilt, the only structural variation allowed in the model is reorientation of the director on the SC tilt cone, i.e. reorientation of the polarization **P**.

The visible transmission spectrum for arbitrary polarizer and analyser positions are calculated using Berreman's method in each slab successively. Interference effects due to finite FLC sample thickness are weak, due to the small reflection coefficients at the FLC–ITO interface. However, they are detectable and they are accounted for in the Berreman method. In the limit that interference effects can be neglected, one could use a simpler technique, such as the Jones Calculus approximation, to calculate the light propagation. This method, which has been applied successfully to several liquid crystal systems [14, 22], has the advantage of being considerably quicker than Berreman's method but applies only for normally incident light and is in general less versatile.

To determine the thickness of a LC cell which has the molecules oriented uniformly, parallel to the glass plates (or indeed the thickness of any appropriately oriented, uniformly birefringent material) one can calculate the normalized transmitted light intensity using the well-known formula

$$\frac{I}{I_0} = \cos^2(\phi_P - \phi_A) - \sin 2\phi_P \sin 2\phi_A \sin^2\left(\frac{\pi \Delta n d}{\lambda}\right), \tag{4}$$

where ϕ_P and ϕ_A are respectively the angles between the optic axis (OA), which is taken to coincide with the molecular director, and the polarizer and analyser. This result takes account only of the relative phase shift between the ordinary and extraordinary rays in the LC materials and ignores reflection. The simple shape and well-defined minima of the spectrum given by this equation provides a way of measuring the thickness of uniform cells with a high degree of accuracy if the birefringence of the material is known.

The optical model computer program assumes that the FLC is sandwiched between two semi-infinite, isotropic slabs of glass with flat parallel faces. In order to measure only what the LC material itself does to the light, we normalize the experimental data, dividing the spectrum of the FLC cell by that of the light source, after subtracting the background signal, or dark count, from each of these. To obtain the source spectrum, we remove the FLC cell and insert an oil-filled cell made with the same ITO glass into the optical path. In this way we hope to duplicate any reflection losses in the real FLC cell at its glass-air and glass-ITO interfaces. Different reflections at the ITO-oil interfaces are minimized by using an oil which is approximately index-matched to the FLC. The relative thickness of the oil layer ($\approx 10\,\mu$m) eliminates interference effects between the bounding plates of the oil cell during the normalization process. We do *not* want to null this interference out of final FLC spectra because it is explicitly included in the optical model.

The modelling program we have developed is extremely flexible and can compute the spectrum of light transmitted through a uniaxial medium with arbitrary variation of the OA orientation along one direction. To generate a very good model spectrum for a $10\,\mu$m thick FLC cell takes about twenty minutes on an IBM PC-XT with arithmetic coprocessor. This is for a calculation of the transmitted intensity at 100 wavelengths using 100 numerical strata and going to 14th order terms in the

exponential expansion used by Berreman in his solution of Maxwell's equations. An adequate model can be obtained with only 15 wavelengths and a 10th order expansion in about one-tenth of this time.

3. Experimental considerations

In this section we describe the physical apparatus and the experimental techniques we use to obtain the transmission spectra of FLC cells. We have developed a sophisticated and versatile instrument that allows us to collect experimental spectra, compute complicated models and display the results with ease. The spectrometer instrument comprises a diffraction grating spectrometer assembly mounted on a microscope and interfaced to an IBM PC-XT with arithmetic coprocessor, as shown schematically in figure 6.

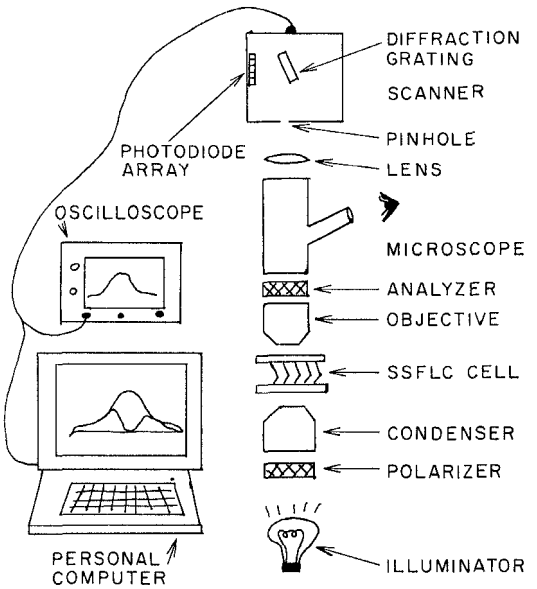

Figure 6. Schematic diagram of the FLC spectrometer. The instrument is a diffraction grating spectrometer mounted on an optical polarizing microscope and interfaced to a personal computer. The pc is used to take experimental data, compute model FLC structures and the associated model transmission spectra, and display all of the data in the form of graphs and easily editable files.

3.1. *Spectrometer*

The FLC cell is placed in a temperature-controlled oven (Instec Inc.) mounted on a Nikon Optiphot polarizing microscope set up for transmission microscopy. Light emerging from the camera port of the microscope is collected by a lens ($f \sim 10$ cm) and focused on the entrance pinhole of a CE395 Fast Spectral Scanner (Spectron Instrument Corp.). Inside the scanner, the beam is directed to a diffraction grating, which disperses it onto a linear, 256 element photodiode array (Reticon 256G). The nominal range is 375–725 nm and the resolution of the photo-diode array approximately 1 nm per elment. This chip produces a smoothed voltage vs. time signal proportional to the integrated light intensity sensed by each element. In the free-running mode, the Scanner produces a new scan of the photodiodes every 1/60 s,

which can conveniently be displayed on an oscilloscope. One can also obtain the result of a signal scan on demand, and in this way our personal computer can read in spectral data in a synchronous fashion. We use an 8-bit A–D converter (Lab Tender interface card from Scientific Solutions Inc.) to digitize the scan. Finally, we average ten such successive scans to improve the signal-to-noise ratio and store the result as the experimental spectrum. The spectral signal is calibrated using laser lines and narrow band interference filters as references. The diffraction grating appears to disperse the light onto the photodiode array with negligible non-linearity (i.e. a plot of array element vs. wavelength is linear).

3.2. *Taking data*

To obtain a normalized transmission spectrum of an FLC cell, we take the ratio of the original FLC (or FILM) spectrum to that of the illuminating soure (SOURCE), after subtracting from each the dark count or background (BACK) spectrum, i.e.

$$I(\lambda) = \frac{(\text{FILM} - \text{BACK})}{(\text{SOURCE} - \text{BACK})}.$$

This is illustrated in figure 7.

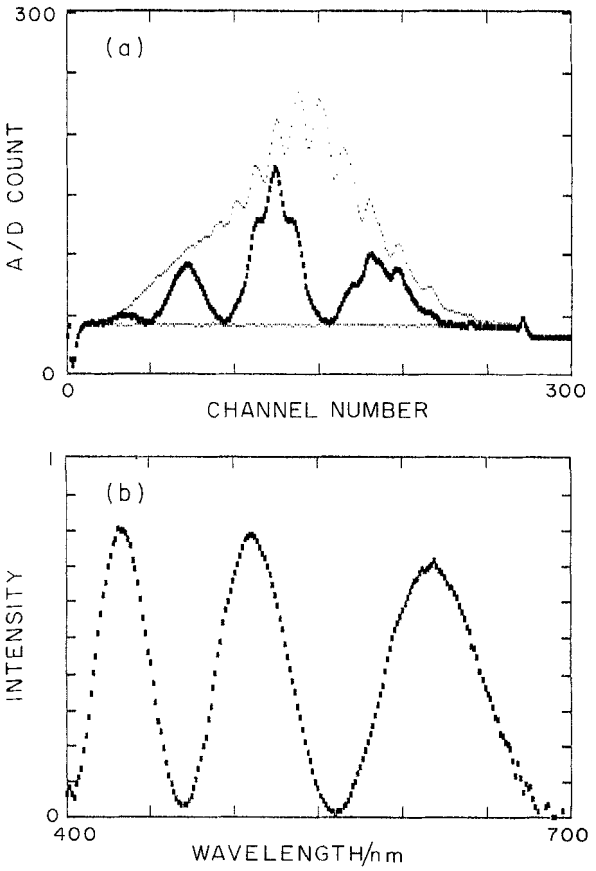

Figure 7. Raw spectral data (*a*) and the corresponding normalized spectrum (*b*).

The spectra are taken using Köhler illumination, with the aperture stop (at the condenser) closed down as much as possible in order to keep the light incident on the FLC cell collimated. This is done because the transmission depends on the incident angle and we prefer to limit our model calculations to a single angle for simplicity. The size and position of the field stop aperture (which is in the focal plane of the sample in Köhler illumination) determine the illuminated area of the cell. BACK spectra are taken with no light entering the Scanner. The level of the dark count is a strong function of the operating temperature of the instrument, the signal doubling about every 10°C near room temperature [23].

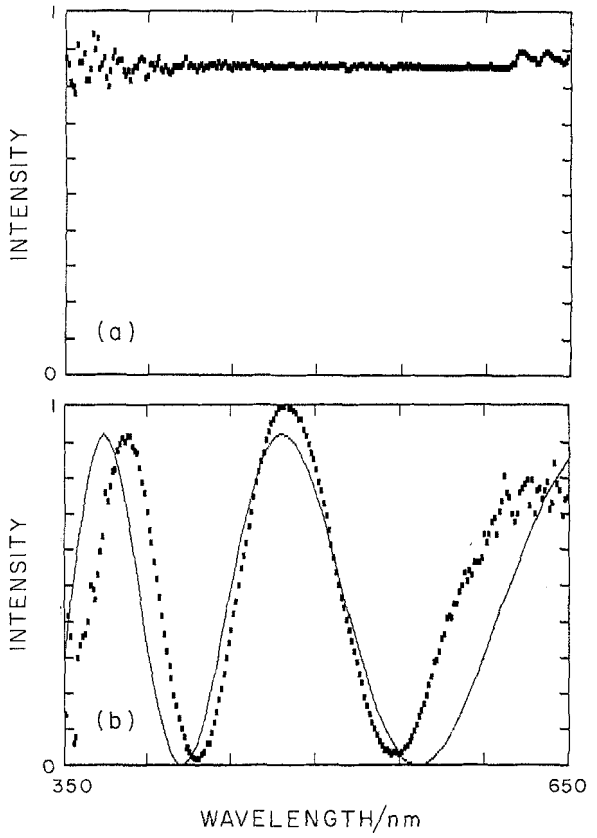

Figure 8. Sample experimental spectra from simple systems: (*a*) a glass microscope slide; (*b*) a quartz wedge oriented at 45° between crossed polarizers (Δn = 0·09, thickness $d \approx 187\,\mu$m. The model spectrum in (*b*) was calculated using equation (4) with $\phi_P = 45°$ and $\phi_A = -45°$. The fit to the quartz spectrum could be improved by accounting for dispersion, in Δn.

As illustrations of typical early results, we show in figure 8 the normalized spectra of a glass microscope slide and of a sample of quartz oriented at 45° between crossed polarizers. We ascribe the poorness of the model fit to the quartz spectrum to dispersion of the refractive index, an effect which was not included in the calculation shown here. In general we found that the best experimental spectra could be obtained using a bright illumination source and short integration times, and by closing the condenser aperture down as much as possible.

3.3. *Refractive index dispersion*

Although there have, to our knowledge, been no comprehensive measurements of the variation of refractive index with wavelength in the FLC material we used, the data available for similar FLC mixtures indicates that there is considerable dispersion of the birefringence Δn, especially at short wavelengths (see, for example, Hark *et al.* [24]). This sort of evidence, combined with our inability to model the spectrum of a smectic A (SA) cell (supposedly a simple, uniformly birefringent slab) in any convincing way *without* dispersion, persuaded us to include dispersion in our subsequent model calculations of FLC cells. We followed the prescription applied to nematics by Wu [25] in which, in the simplest approximation, the variation of the LC birefringence is given by

$$\Delta n(\lambda) = G \frac{\lambda^2 \lambda_*^2}{\lambda^2 - \lambda_*^2}, \tag{5}$$

where G is a temperature dependent amplitude and λ_* is the (mean) wavelength of the first UV absorption band below the visible part of the spectrum

The main effect of dispersion is to push the spectral peaks closer together. In figure 9 we show how including dispersion enabled us to obtain a good fit to the spectrum of a SA cell. Without dispersion the spectral minimum was simply too broad (or too narrow, if the model cell thickness was increased enough to move to the next

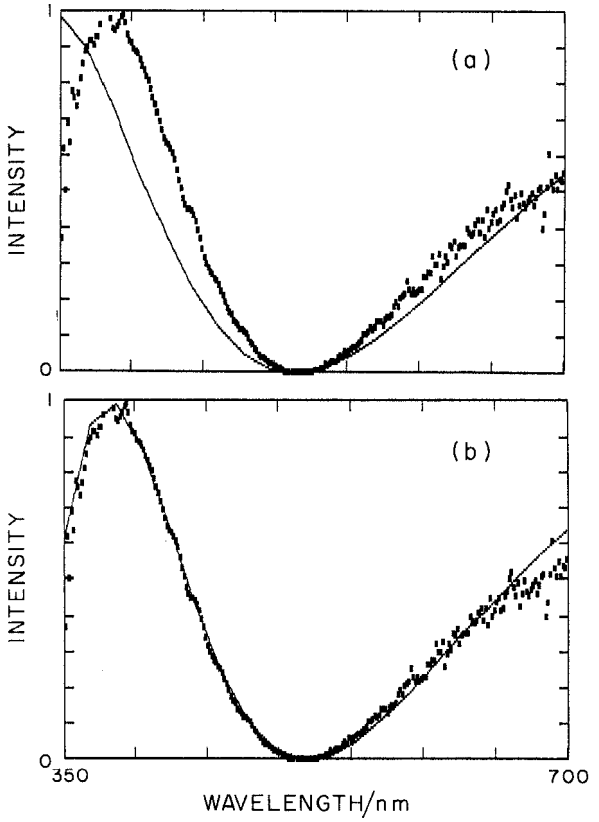

Figure 9. The effect of including dispersion of the birefringence on the model spectrum of an FLC in the SA phase. The experimental spectrum is of a SA cell oriented with the average director orientation (i.e. the OA) at 45° between crossed polarizer and analyser. The model spectra were calculated (*a*) with constant Δn, and (*b*) including the effects of dispersion. The fit with dispersion is much better.

'fringe'). This same cell formed a splayed chevron structure when cooled to the SC phase and was used to obtain the spectral data presented in the rest of this chapter. We used a birefringence ranging between 0·13 and 0·14 over the visible region, as shown in figure 10. We assumed an ordinary index of $n_o = 1{\cdot}49$ and a refractive index for the cell glass of $n_g = 1{\cdot}50$, the model spectra being quite insensitive to small variations in these parameters.

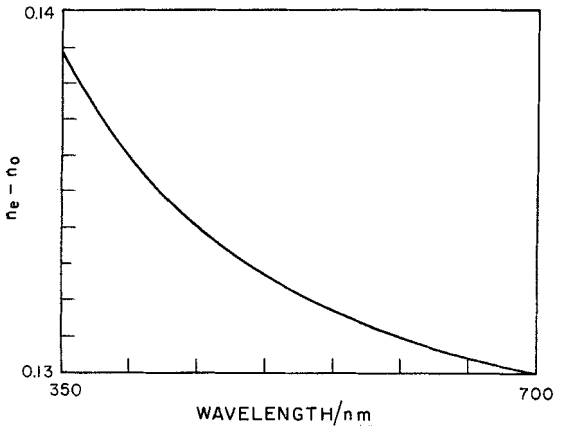

Figure 10. Dispersion of the Δn, the optical birefringence, as a function of wavelength. This plot shows the dispersion curve $\Delta n(\lambda)$ as used in the model calculations of chevron cell spectra. The curve is obtained using Wu's formula (equation (5)) with fixed points Δn (422 nm) = 0·135 and Δn(700 nm) = 0·13.

3.4. *Fundamental experimental observations*

Our cells were made by placing two ITO-coated glass slides, cleaned in methanol, face to face with dilute particle spacers. The gap between the plates is filled with LC material, drawn in by capillary action in the isotropic phase. While cooling into the SA, the cell is gently sheared [26], which aligns the smectic layers along the shearing direction and results in a homogeneous texture with few visible defects. The glass plates favor planar orientation of the directors and upon cooling into the SC phase the layers adopt the chevron geometry. The cells are thin enough that there are no helix lines present. We use a mixture of W7-W82 [27] which has a SA–SC phase transition at about 50°C and is in the SC phase at room temeprature, where we took our data.

Using this technique, we can prepare cells that are homogeneous over quite large areas (e.g. 100 μm × 100 μm). In a well aligned cell, the UP and DOWN regions can be distinguished by their birefringence colours, which appear to nearly interchange, but never extinguish, when the cell is rotated. In the absence of applied field, both types of domain can coexist in the cell, separated by sharp domain walls as shown in the photographs of figure 11. Two domains with the same average polarization, on the other hand, can be separated by a zig-zag defect, in which case they have similar colour but differ in intensity. It is precisely these distinctive colours that we use to test our model of director structure in these cells.

Applying a small field first causes the domains favoured by the sign of the field to grow, typically by the motion of boat-shaped domain walls along the chevron interface [28, 29]. After the domain walls have swept through the sample, increasing the field further results in an additional, more continuous colour change, as the polarization in the sample aligns more closely with the **E** field. At high field, the entire

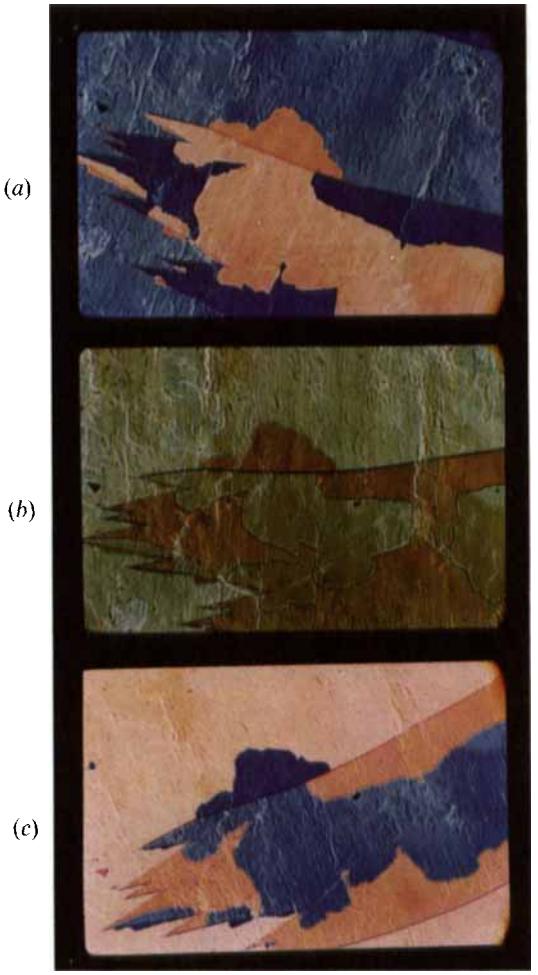

Figure 11. Typical features of splayed chevron cells. The photograph shows three views of a splayed chevron cell at zero field paced between crossed polarizers. The projection of the layer normal is along the polarizer in the middle frame (*b*) ($\alpha = 0$, cf. figure 12) and is rotated to an angle of (*a*) $\alpha = -20°$ and (*c*) $\alpha = +20°$ on either side. In the pictures, we can see most of a closed zig-zag defect loop, which appears as a dark black line. In (*a*) the UP regions are pink and the DOWN regions blue. The UP and DOWN domains nucleate mainly at the zig-zags and are separated by distinct domain walls which can be driven laterally by applied fields. For $\alpha \neq 0$ the intensity of domains with the same average polarization is different on opposite sides of the zig-zag because inside the loop the chevron interface is located 28 per cent of the way up the cell, while outside it is at 72 per cent. When the cell is rotated through any angle α', the colours of the UP and DOWN domains nearly interchange relative to those for $-\alpha'$, as can be seen by comparing frame (*a*) with frame (*c*).

sample is almost uniform and can finally be rotated to a position where there is reasonable extinction.

In order to compare spectral data of the cell with a model, one needs to determine quite carefully how the smectic layers are oriented relative to the polarizer and analyser. For normally incident light, the actual direction of layer bend in the chevron is irrelevant, since rotating the cell by 180° about the incident beam results in an optically indistinguishable situation. Only the chevron axis (i.e. the projection of the layer normal on the glass plates) needs to be known. In addition, a change in intensity

as a zig-zag wall is crossed indicates that the chevron interface is located asymmetrically in the cell.

The sign of the polarization **P** and the orientation of the layer normal can be determined by applying electric fields to the cell. The SC tilt angle θ is more easily measured in a uniform SSFLC cell, where better extinction can be obtained. The material we used has positive polarization, i.e. $\hat{z} \times \hat{n} \sim +\hat{\mathbf{P}}$. We used $\theta = 22°$ and a layer tilt of $\delta = 18°$, which are consistent with the X-ray results of Rieker and Clark in similar cells. [2, 3] The model spectra turn out to be relatively insensitive to the exact values of these angles.

The illuminating light is assumed to be normally incident on the cell, which is placed horizontally on the microscope table. Angular rotations of the cell about the incident beam are described by α, which is the angle between the projection of the layer normal onto the glass plates (the chevron axis) and the polarizer, with α increasing couter-clockwise when viewed from above as shown in figure 12. As an example, if a large positive (DOWN) field were applied to the cell then a rotation of $\alpha \approx -\theta$ would align the average director orientation with the polarizer; for a negative (UP) field this would require a rotation of $\alpha \approx +\theta$. With the cell between crossed polarizers, there is a four-fold rotational symmetry about the cell normal and the cell appears the same when rotated in increments of 90°.

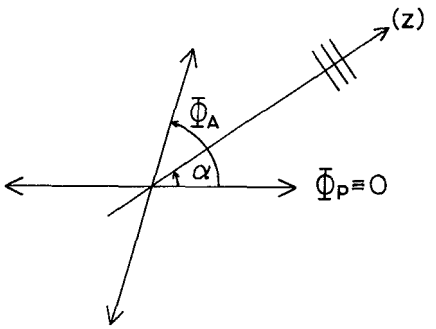

Figure 12. Rotational geometry of the FLC cell. The view here is looking down on the cell, just as one would through the microscope. The projection of the layer normal onto the glass plates ($\hat{z}$) makes an angle α with the polarizer. The analyser angle Φ_A is also measured counter-clockwise from the polarizer axis.

4. Optical properties of splayed chevron cells

In this section, we will discuss the optical properties of chevron cells in detail and make some general statements about what they do to polarized light. Although a splayed chevron cell can not, in general, be rotated to extinction between crossed polarizers, it is possible, after rotating the analyser slightly away from the crossed position, to orient the cell so that hardly any light comes through, as shown in the photographs of figure 13. This distinctive optical property is a direct result of the cell's non-uniform director structure but can not, as one might at first suppose, be explained by simple analogy with the 'Mauguin limit' propagation of twisted nematic (TN) cells. In TN cells, if the incident light is polarized along the optic axis at the bottom of the cell (OA_b) and the OA changes direction sufficiently slowly, then the polarization of the light can be rotated adiabatically and light emerges at the top of the cell still polarized along the OA. The twisted nematic director structure then acts as a kind of optical polarization waveguide [32].

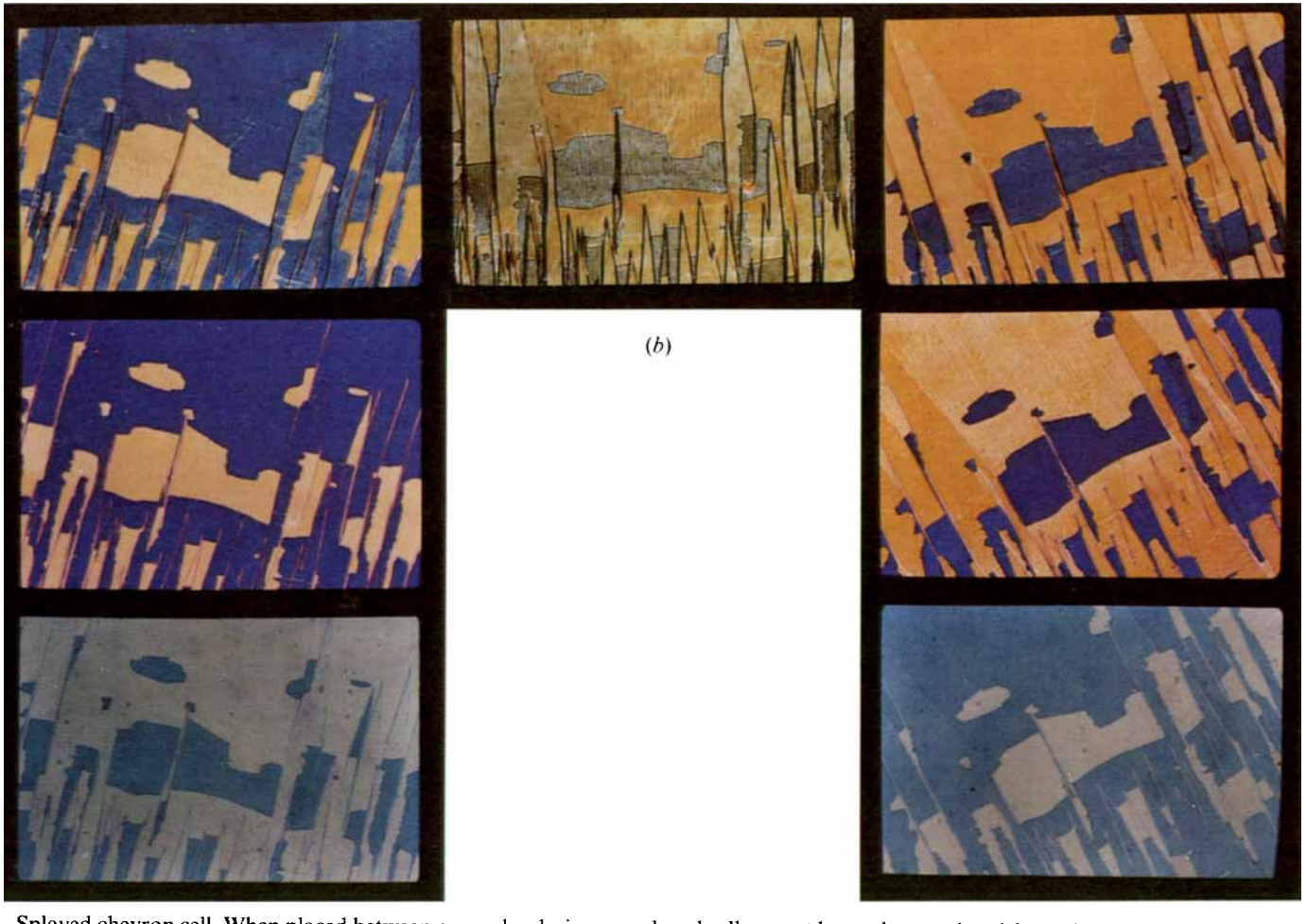

Figure 13. Splayed chevron cell. When placed between crossed polarizers a splayed cell cannot be made to extinguish, as shown in (*a*)–(*c*). However, when the polarizer angle is reduced from $\Phi_A = 90°$ to $\Phi_A \approx 70°$ as in (*d*) and (*e*), then the transmitted light is largely extinguished. Subsequently rotating the analyzer by 90° to $\Phi_A = 160°$, as in (*f*) and (*g*), allows a lot of light through the cell.

In splayed chevron cells, the director orientation also varies smoothly through the cell, with the projection of the OA on the plates being twisted through an angle that approaches twice the SC tilt angle as the layer tilt goes to zero but is in general less than this in cells with pretilted surface polarizations and tilted layers. We have found, through our calculations and observations, however, that the light propagation in a typical thin chevron SSFLC cell is more complicated than in a simple twisted nematic and does not satisfy the Mauguin limit in most situations of SSFLC use.

4.1. *Phase retardation by SSFLC birefringence*

As we have seen, a typical chevron cell comprises both uniform and splayed parts. In order to gain some insight into the fundamental optical properties of this arrangement, we begin by considering what happens to light which is linearly polarized at some arbitrary angle and is normally incident on a uniform, birefringent medium such as the SSFLC structure shown in figure 14 (*a*). As the light travels through the medium, the polarization becomes elliptical, with the principal axis of the polarization ellipse rotating back and forth through the OA at a rate which is coupled to the phase shift between the ordinary and extraordinary components of the polarization, given by $\Phi = 2\pi\Delta n x/\lambda$, where x is the distance travelled by the light ray. For example, a birefringent slab that is just thick enough to have a phase shift of $\Phi = 180°$, thereby rotating the plane of polarization so that the outgoing polarization appears to be a mirror reflection of the incident polarization through the OA, is a 'half-wave ($\lambda/2$) plate'.

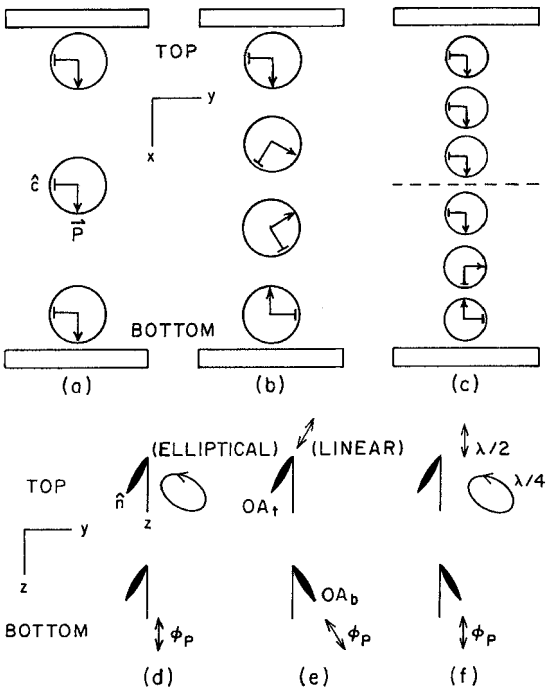

Figure 14. Light propagation in simple director structures. SSFLC cell with (*a*) uniform state; (*b*) uniformly splayed state; (*c*) splayed-uniform regions separated by an internal interface. The layers are normal to the glass plates and there is no pretilt of the polarization at the boundaries. In (*d*)–(*f*) we show the projections of the OA at the top and bottom plates of the cell. Notice that states (*b*) and (*c*) have the same orientation of the OA at the boundaries. In (*f*) we show two different final polarization states corresponding to Mauguin propagation through cells of different thickness.

In a non-uniform region, like the splayed part of a chevron cell, the transmitted polarization is not only determined by the birefringence but also by the reorientation of the OA in the cell. In order to evaluate these effects we will initially ignore the smectic layer tilt, but we will consider the effect of an internal interface.

4.2. *Mauguin limit*

In figure 14(*b*) and (*c*) we show two splayed states. State (*b*) is uniformly splayed, while state (*c*) has an internal interface which confines the splay to the lower half of the cell, leaving the upper half uniform. Since the orientations of the OA at each glass plate are the same in each case, in the Mauguin limit the two arrangements would be optically identical. In this limit, incident light linearly polarized along the OA at the bottom of the cell (OA_b) remains linearly polarized and leaves the cell polarized along the OA at the top (OA_t), as shown in figure 14(*e*). If the incident light is polarized instead along the layer normal, as in figure 14(*f*), then the exiting beam is in general elliptically polarized. The final polarization state can be found in this instance by resolving the incident polarization into components parallel and perpendicular to the beginning director, rotating these components *à la* Mauguin, recombining the result and then phase shifting the ordinary and extra-ordinary components (referred to OA_t) by an amount appropriate to the cell thickness. For example, a 180° phase shift would leave the exiting polarization linear and along the same direction as the incident polarization, as shown in figure 14(*f*).

For the sake of simplicity, we will ignore in our discussion the effects of changes in the elevation angle of the OA measured relative to the glass plates that occur as the director precesses on its tilt cone. We imagine instead that there is pure twist of the director between the bottom and the top of the cell. This is a reasonable approximation in chevron cells at zero field, where the directors really do remain almost parallel to the boundaries as they precess between the two allowed pretilted states.

In order to determine when the Mauguin limit is satisfied in SSFLCs, we have calculated the ellipticity of initially linearly polarized light propagated though various slabs of FLC material whose thickness will be seen to correspond to that of the real chevron cell studied later but which have simpler director structures so that we can intrepret the results more easily. All of the calculations in this section include the effects of dispersion of the birefringence, with Δn as shown in figure 10, and we use $\theta = 22°$.

4.3. *Uniform cell*

We first consider what happens to light in a 3·9 μm thick, uniformly oriented cell, such as the one shown in figure 14(*a*). If the input polarization is along the layer normal, as shown in figure 14(*d*), then the state of the output polarization is as summarized in table 1(*a*). In all of the tables, E_e and E_o, which are the amplitudes of the extraordinary and ordinary components of the transmitted electric field, are referred to the OA at the top of the cell (i.e. OA_t). Φ is the relative phase of the two components and the orientation angle ω of the major axis of the polarization ellipse can be calculated using the expression [30]

$$\tan 2\omega = \frac{2E_e E_o}{E_e^2 - E_o^2}\cos\Phi, \tag{6}$$

where ω is measured in the usual counter-clockwise sense from OA_t.

The data in table 1 (*a*) show that the output light is linearly polarized at two wave lengths. At about 500 nm the cell is a full-wave (λ) plate, with a phase shift $\Phi = 2\pi$ and a polarization azimuth of $\omega = 22°$, which is the same as the input polarization. At about 360 nm the cell is a one-and-a-half wave plate, with $\Phi = 3\pi$ and $\omega = -22°$, which is a reflection of the input polarization through the OA.

4.4. *Uniformly splayed cell*

Next we consider a uniformly splayed cell of the same thickness (3·9 μm), as illustrated in figure 14 (*b*). When the input polarization is along OA_b then the output polarization is as shown in table 1 (*b*). By comparing this with the uniform case (table 1 (*a*)) we see that the splay has effectively halved the birefringence, with the cell at 500 nm now looking like a half-wave ($\lambda/2$) plate ($\Phi = \pi$) and at 1000 nm approaching a quarter-wave ($\lambda/4$) plate ($\Phi = \pi/2$).

The principal axis of the polarization ellipse ω varies between 0° and about $-15°$ over the range of wavelengths shown. At very short wavelengths, the light is essentially polarized along the optic axis OA_t, the depolarized component E_0 being less than 10 per cent of the total and $\omega \approx 0$. This means that the Mauguin limit is obeyed at the shortest wavelengths only, with the propagation deviating more and more from the waveguide mode with increasing wavelength.

The output polarization was calculated for several uniformly splayed cells with the same director structure as in this example but using different values of Δn and d. The results suggest that we can postulate a criterion for when the depolarization is less than 10 per cent and the Mauguin limit is obtained. In splayed cells in which the director twists through about 45°, the LC structure acts as a waveguide for wavelengths

$$\lambda_c < \tfrac{2}{3}\Delta n d,$$

or, equivalently,

$$\Phi_c > 3\pi,$$

which says that, as a rule of thumb, the Mauguin limit is only obeyed in splayed cells which are one-and-a-half wave plates or thicker. This can be compared with Mauguin propagation in twisted nematics, which occurs, according to Chandrasekhar [31], when the optical phase shift per imaginary stratum of the LC is much less than twice the rotation of the OA in the stratum. Extrapolating this to an idealized chevron cell of the type shown in figure 14 (*b*) or (*c*) would require $\Phi > 4\theta$, or $\Phi > \pi/2$ in our case. De Gennes, on the other hand, says that the adiabatic approximation is obtained in cholesterics of pitch p when λ is much less than Δnp, which corresponds to $\Phi = 2\pi\Delta nd/\lambda$ much greater than 2π. Both results are in general agreement with ours.

4.5. *Splayed cell with internal interface*

Finally, we consider how light is propagated through a 3·9 μm cell with an internal interface which divides it into a uniform and a splayed slab each 1·95 μm thick, as shown in figure 14 (*c*). The input polarization is once again along OA_b and the output is shown in table 1 (*c*).

With this director structure, the cell is a full-wave (λ) plate at about 400 nm and a half-wave ($\lambda/2$) plate at about 775 nm. There is no Mauguin propagation at any

Table 1. (*a*) Transmitted polarization state for incident light linearly polarized along the layer normal in a uniformly aligned cell 3·9 μm thick and a tilt angle $\theta = 22°$. (*b*) Transmitted polarization for incident light linearly polarized along the director (OA_b) at the bottom of a uniformly splayed 3·9 μm cell, as shown in figure 14 (*b*). (*c*) Transmitted polarization for incident light linearly polarized along the director (OA_b) at the bottom of a 3·9 μm cell which is divided into uniform and uniformly splayed parts by an internal interface half way up the cell, as shown in figure 14 (*c*). (*d*) Transmitted polarization for incident light linearly polarized along the director (OA_b) at the bottom of a 7·8 μm cell which is divided into uniform and uniformly splayed parts by an internal interface half way up the cell, as shown in figure 14 (*c*). (*e*) Transmitted polarization for incident light linearly polarized along the director (OA_b) at the bottom of a 3·9 μm cell with chevron layer structure which is divided into uniform and uniformly splayed parts by an internal interface half way up the cell, as shown in figure 4 (*f*). (*f*) Transmitted polarization for incident light linearly polarized along the director (OA_b) at the bottom of a 3·6 μm chevron cell with the director structure used to model the spectral data shown in figure 15. Phase shift Φ is in degrees, restricted to the range $-180°-+180°$.

Index	λ (nm)	E_e	E_o	Φ	E_e	E_0	Φ	E_e	E_o	Φ	E_e	E_o	Φ	E_e	E_o	Φ	E_e	E_o	Φ
1	350·0	0·925	0·375	−163·1	0·997	0·077	−97·2	0·894	0·454	58·0	0·994	0·072	99·3	0·992	0·142	60·3	0·991	0·111	33·1
2	372·4	0·927	0·375	157·9	0·992	0·115	−114·5	0·878	0·482	29·7	0·994	0·110	43·1	0·987	0·173	31·3	0·988	0·129	5·2
3	394·8	0·927	0·375	124·3	0·988	0·153	−129·3	0·864	0·505	5·2	0·989	0·148	−5·35	0·981	0·199	6·2	0·987	0·146	−18·7
4	417·2	0·925	0·375	95·0	0·980	0·190	−142·2	0·850	0·524	−16·4	0·980	0·184	−47·6	0·973	0·221	−15·6	0·987	0·160	−39·5
5	439·7	0·926	0·375	69·0	0·972	0·224	−153·6	0·840	0·542	−35·3	0·973	0·218	−84·7	0·970	0·242	−34·9	0·982	0·172	−57·7
6	462·1	0·925	0·375	46·2	0·965	0·257	−163·6	0·826	0·556	−52·2	0·966	0·251	−117·7	0·963	0·259	−51·1	0·981	0·183	−73·9
7	484·5	0·927	0·375	25·7	0·958	0·287	−172·7	0·822	0·569	−67·4	0·959	0·281	−147·3	0·961	0·275	−67·4	0·981	0·193	−88·4
8	506·9	0·927	0·375	7·1	0·949	0·314	179·2	0·824	0·580	−81·1	0·950	0·309	−173·9	0·957	0·289	−81·3	0·979	0·201	−101·7
9	529·3	0·927	0·375	−9·7	0·940	0·339	171·8	0·807	0·590	−93·5	0·941	0·334	162·0	0·954	0·301	−93·8	0·978	0·208	−113·1
10	551·7	0·927	0·375	−24·9	0·931	0·363	165·1	0·801	0·598	−104·9	0·932	0·358	140·0	0·950	0·311	−105·2	0·986	0·215	−123·8
11	574·1	0·927	0·375	−38·8	0·923	0·384	158·9	0·795	0·606	−115·3	0·925	0·380	119·9	0·947	0·321	−115·7	0·973	0·220	−133·6

12	596·6	0·926	0·375	−51·5	0·914	0·403	153·2	0·790	0·612	−124·8	0·915	0·398	101·4	0·973	0·329	−125·3	0·972	0·225	−142·6
13	619·0	0·925	0·375	−63·3	0·905	0·421	147·9	0·784	0·617	−133·6	0·908	0·417	84·4	0·839	0·336	−134·2	0·973	0·230	−150·9
14	641·4	0·925	0·375	−74·4	0·897	0·437	143·0	0·781	0·623	−141·8	0·899	0·433	68·6	0·937	0·344	−142·4	0·971	0·234	−158·6
15	663·8	0·927	0·375	−84·4	0·891	0·453	138·4	0·778	0·628	−149·4	0·893	0·449	53·9	0·936	0·350	−150·0	0·969	0·237	−165·7
16	686·2	0·925	0·375	−93·7	0·883	0·466	134·1	0·773	0·632	−156·5	0·885	0·463	40·2	0·932	0·355	−157·1	0·970	0·241	−172·3
17	708·6	0·926	0·375	−102·6	0·877	0·479	130·1	0·771	0·636	−169·1	0·877	0·475	27·4	0·932	0·361	−163·7	0·967	0·244	−178·5
18	731·0	0·926	0·375	−110·7	0·870	0·491	126·3	0·767	0·639	−169·3	0·871	0·487	15·5	0·929	0·365	−169·9	0·969	0·247	175·8
19	753·4	0·926	0·375	−118·5	0·862	0·502	122·8	0·765	0·643	−175·1	0·865	0·498	4·2	0·928	0·370	−175·7	0·966	0·249	170·4
20	775·9	0·926	0·375	−125·6	0·858	0·512	119·4	0·762	0·646	179·5	0·859	0·508	−6·3	0·256	0·373	178·9	0·968	0·252	165·3
21	798·3	0·926	0·375	−132·5	0·852	0·521	116·2	0·760	0·649	174·3	0·853	0·518	−16·3	0·925	0·377	173·7	0·965	0·253	160·5
22	820·7	0·925	0·375	−138·8	0·846	0·529	113·3	0·757	0·651	169·5	0·848	0·527	−25·7	0·922	0·380	168·9	0·966	0·256	156·0
23	843·1	0·927	0·375	−144·9	0·843	0·538	110·4	0·756	0·654	164·9	0·844	0·535	−34·6	0·923	0·384	164·3	0·966	0·258	151·8
24	865·5	0·925	0·375	−150·7	0·836	0·545	107·7	0·753	0·655	160·5	0·839	0·543	−43·0	0·920	0·386	159·9	0·963	0·259	147·7
25	887·9	0·926	0·375	−155·9	0·833	0·552	105·1	0·752	0·657	156·4	0·833	0·549	−51·0	0·920	0·389	155·8	0·965	0·261	143·9
26	910·3	0·927	0·375	−161·3	0·828	0·559	102·7	0·751	0·659	152·5	0·829	0·556	−58·6	0·920	0·392	151·9	0·964	0·262	140·3
27	932·8	0·925	0·375	−1661·	0·823	0·564	100·3	0·748	0·660	148·8	0·826	0·563	−65·8	0·917	0·393	148·2	0·962	0·263	136·9
28	955·2	0·926	0·375	−170·7	0·820	0·571	98·1	0·748	0·660	145·3	0·821	0·568	−72·7	0·917	0·396	144·7	0·963	0·265	133·6
29	977·6	0·927	0·375	−175·2	0·817	0·576	96·0	0·747	0·664	141·9	0·818	0·574	−79·3	0·917	0·398	141·3	0·964	0·266	130·5
30	1000·0	0·925	0·375	−179·5	0·812	0·580	93·9	0·745	0·665	138·7	0·814	0·579	−85·5	0·915	0·399	138·1	0·962	0·266	127·5
			(*a*)			(*b*)			(*c*)			(*d*)			(*e*)			(*f*)	

wavelength, presumably because the distortion of the director is now tightly confined to one half of the cell and the polarization is unable to follow the twist of the OA.

If we double the cell thickness ($d = 7{\cdot}8\,\mu$m) without changing the director orientations at the boundaries, then the splayed region is once again spread over 319 μm and the Mauguin limit is obeyed at the very shortest wavelengths (see table 1 (*d*)), just as it was in the uniformly splayed 3·9 μm cell (table 1 (*b*)). The retardance of the cell scales simply with thickness, the optical thickness of the 7·8 μm cell being 2λ at 390 nm, $3\lambda/2$ at 510 nm, λ at 755 nm and $3\lambda/4$ at 1000 nm.

In an idealized splayed chevron cell with tilted layers, though, the surface polarization pretilt reduces the total amount of polarization splay and hence the total twist of the director. If the splay is confined to the thicker 'half' of an asymmetric chevron, which it would necessarily be either in the UP or in the DOWN state, this can relax the Mauguin Criterion given earlier, since the director will twist more gradually than in our examples with normal layering and no pretilt. For example, in a cell with $\theta = 22°$ and $\delta = 18°$ the apparent tilt angle (i.e. half the projection of the tilt cone onto the bounding glass plates is only about 13°, so the director projection in an idealized chevron cell with planar orientation at the glass plates would rotate through an angle of about 26° (as compared with 44° in our earlier examples). If we propagate light though such a cell 3·9 μm thick with a symmetric chevron and the incident beam polarized along OA_h as usual, then we see from the data in table 1 (*e*) that the depolarization at 350 nm is down to about 14 per cent, which is much less than in the example with normal layering shown in table 1 (c) and is closer to the 10 per cent level which we use as the criterion for Mauguin propagation.

4.6. *Optical extinction in a real cell*

To study experimentally the circumstances under which a splayed chevron cell gives extinction in the absence of applied field, we obtained the transmission spectra of an SSFLC cell in the extinction position and rotated by 30°, 60° and 90° from this orientation. The analyser was oriented at 72° with respect to the polarizer and reasonable extinction was obtained for $\alpha = 10°$. We measured the transmission spectrum in both UP and DOWN states and calculated model spectra based on the generic structures presented earlier, assuming for simplicity that the chevron interface was located in the middle of the cell. The surface polarization orientations were adjusted to obtain a reasonable fit at the initial orientation and then left unchanged for the rest of the calculations, the only variable parameter being α. The models are in excellent qualitative agreement with the experimental data and are shown in figure 15.

The model surface director orientations that successfully fitted the experimental data did yield the fundamentally important piece of information that in this cell the polarization **P** points *into* the bulk FLC, i.e. $\hat{P} \cdot \hat{s} < 0$. This finding is in agreement with an independent optical experiment on a similar cell recently performed by Xue *et al.* [13]. (We note that although it is possible to obtain some reasonable fits of the data assuming $\hat{P} \cdot \hat{s} > 0$, the SC model cell thickness necessary in this case is inconsistent with that deduced from the clearcut SA spectrum, being a whole micron greater.)

The cell is a dark purple colour at extinction and an examination of the spectrum shows that this is due to the elimination of the wavelengths in the middle of the visible range. Since a typical incandescent light source produces a lot of yellow light, and the

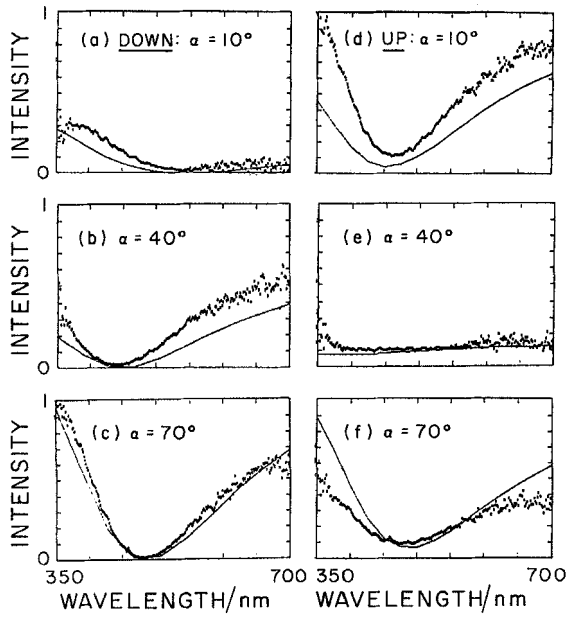

Figure 15. Transmission spectra of an 'extinguishing' chevron cell. The plots show the spectra of both UP and DOWN domains at zero field. The experimental spectra were obtained with the polarizer at $\Phi_A = 72°$ to the polarizer. The cell was initially oriented for extinction in the DOWN state (at $\alpha = 10°$) and then rotated in increments of 30°. The spectra at 90° would be identical to those at 0°. The spectra are of the DOWN state (*a*, *b*, *c*) and the UP state (*d*, *e*, *f*). the models have a cell thickness $d = 3{\cdot}6\,\mu m$ and a chevron interface exactly in the middle of the cell.

human eye is most sensitive to these wavelengths anyway, their elimination makes the FLC cell appear particularly dark. The ellipticity of the light propagated though our model cell when the incident polarization is along OA_b appears in table 1 (*f*). These data show that a broad band of visible wavelengths emerge from the cell only slightly elliptically polarized, along an axis that is within $\pm 10°$ of the orientation of OA_t. Since the depolarization is more than 10 per cent, however, we would say that the Mauguin limit is not satisfied in this cell. Changing the polarizer orientation changes the wavelength of light that emerges polarized, as well as its polarization direction. An optical microscopist seeking to obtain 'extinction' in these cells is probably unconsciously just choosing the polarizer, analyser and cell orientations that predominantly reduce the amount of yellow light reaching his eye.

Strictly speaking, the analyser can only eliminate linearly polarized light. Which wavelengths end up being linearly polarized after going through a splayed chevron cell is a sensitive function of the refractive index dispersion, of the cell thickness and of the director orientation of the cell. In our models, a 10 per cent change in thickness or a 20° change in polarizer orientation were sufficient to shift the linearly polarized wavelength by several hundreds of nanometers.

In conclusion, a splayed chevron cell in general changes the polarization of incident light from linear to elliptical and does not act like an optical waveguide of the Mauguin type, except perhaps at very short wavelengths. Nevertheless, considerable apparent extinction of the transmitted light can be achieved by orienting the polarizer and analyzer to eliminate the yellow wavelengths.

5. Director structures in electric fields

Finally, we present the results of measurements of the director structure in a splayed chevron cell as a function of applied electric field. We first obtained transmission spectra at various d.c. voltages, taking care to avoid zig-zags, domain walls and other defects in the sample. We then attempted to fit the data with model spectra calculated using a sequence of director structures that were consistent with our basic model. A series of photographs showing the effect of electric field on the cell appears in figure 16.

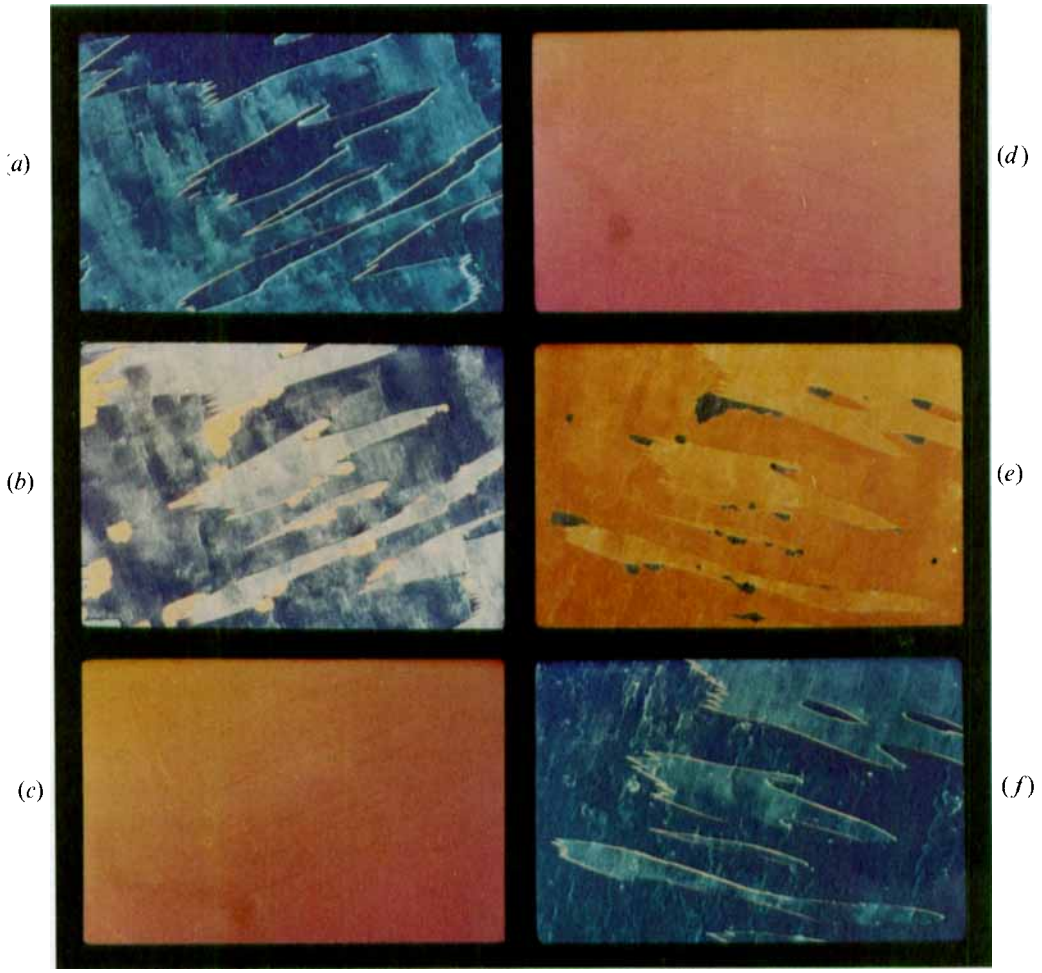

Figure 16. Change of cell appearance with electric field. The photographs show a splayed chevron cell oriented between crossed polarizers at a sequence of different voltages. DOWN domains appear blue and UP domains yellow-pink at this orientation ($\alpha = 20°$). The cell is about 3·9 μm thick.

5.1. *Choice of fitting parameters*

Because so many relevant parameters were not known for this cell, the fitting problem was non-trivial. A reasonable set of parameters that gave a good fit in some circumstances might prove to be totally unacceptable if the field were changed or the

cell rotated. In view of these constraints, the fact the we achieved satisfactory fits of almost all of the spectral data suggests that the chosen set of parameters do reflect the actual state of the cell rather well.

We have already discussed the birefringence, which was chosen to be in the range $0{\cdot}13 < \Delta n < 0{\cdot}14$ over the visible spectrum. This constrained the cell thickness to be about $3{\cdot}9\,\mu$m. We chose the refractive index of the bounding glass plates as $n_g = 1{\cdot}5$ and the ordinary index of refraction of the FLC as $n_o = 1{\cdot}49$. In this cell the chevron was found to be asymmetric, the chevron interface being located about 28 and 72 per cent of the way up the cell respectively on opposite sides of zig-zag defect. We used a SC tilt angle of $\theta = 22°$ and a layer tilt of $\delta = 18°$. In the absence of any independent data, we used a value of $P/K = 1(V\,\mu\text{m})^{-1}$, a number appropriate to that of the FLC DOBAMBC which has a value of **P** and θ nearly that of the W7-W82 mixture studied [16].

Experimental spectra were obtained at three cell orientations, first with the polarizer oriented approximately along the projection of the layer normal and then with the cell rotated by $\pm 20°$ from this position, as shown in figures 11 and 16. The best model fits were achieved by assuming that the projected layer normal was oriented at $\alpha = -2°, -22°$ and $+18°$ from the polarizer. The analyser was crossed with respect to the polarizer in all cases. Having settled on values for all of the other parameters, one is then constrained to vary only the four angles (ϕ) specifiying the polarization direction at the two glass plates and immediately above and below the chevron interface.

5.2. *Results*

The model fits are in general extremely good, with the fitted surface polarization orientations changing in a physically reasonable way with applied field. Model fits were calculated at only 15 wavelengths so they do not always appear as smooth as they really are, especially at shorter wavelengths where Δn increases rapidly. We used about 15 numerical strata per micron of LC material and terms up to 10th order in Berreman's expansion. The results are summarized in table 2.

The experimental data were taken in the order $N1$, $N2$, $N3$,... and so on, and the model structures should be viewed in this light. The aim during fitting was to achieve physically reasonable and self-consistent changes in the surface orientations between strictly consecutive sets of data and this was achieved most of the time. Some inconsistencies between fits obtained at similar field but at different angles (and hence at different times) are direct evidence of hysteresis, an effect which is easily observed near zero field, for example, where the threshold voltage for moving an UP–DOWN domain wall can occur anywhere between $\pm$ 1/2V, depending on the immediate past history of the cell. This is probably caused by temporary accumulations of ionic charge due to impurities in the FLC material and a consequent alternation of the local electric field.

The voltage shown in parentheses with some of the fits is the value that was used in the cases where the equation of motion became numerically insoluble using the true voltage. This occurs near the critical field at which an inflection point first appears in the $\phi(x)$ curve in the splayed part of the cell. For example, in figure 5 (*b*) we could not obtain a solution for $\pm$ 1 V as this was too close to the critical voltage.

In figure 17 are a series of spectra at different fields which show the gradual changes that occur with field in any given domain, and the dramatic change in the spectrum that occurs when a domain wall has passed through the sample, switching

Table 2. Fitted director states in positive fields. This table shows the director structures of a chevron cell obtained by fitting measured transmission spectra at different positive voltages. The acutal spectra for the first column are shown in figure 17. At each voltage we show the values of ϕ at the top of the cell, just above and just below the chevron interface, and at the bottom of the cell. '[poor]' indicates that the spectral fit was poor. Voltages in square brackets were the values used when the director field equation became insoluble using the actual experimental voltage.

Outside zig-zag loop (chevron at 72 per cent)						Inside zig-zag loop (chevron at 28 per cent)					
$\alpha = +18°$		$\alpha = -2°$		$\alpha = -22°$		$\alpha = +18°$		$\alpha = -2°$		$\alpha = -22°$	
N31	+1·9 V	N18	+0·98 V	N25	+1·14 V			N3	+1·51 V	N8	+0·57 V
47°		45°		10°	[poor]			25°	[1·1 V]	45°	
47°		45°		10°				25°		45°	
−47°		−45°		−10°				−25°		−45°	
−70°		−90°		−15°				−75°		−100°	
N30	+0·53 V	N17	+0·53 V			N15	+0·52 V	N2	+0·5 V	N9	+0·18 V
55°		55°				33°		40°		53°	
55°		55°				33°		40°		53°	
−55°		−55°				−33°		−40°		−53°	
−80°		−105°				−73°		−85°		−107°	
N29	+0·14 V			N24	0 V	N14	−0·03 V	N1	0V	N7	0V
60°	[0·07]			60°	[poor]	40°		53°		53°	
60°				60°		40°		53°		53°	
−60°				−60°		−40°		−53°		−53°	
−92°				−100°		−102°		−127°		−105°	
				N23	−0·41 V					N10	−0·17 V
				80°	[poor]					55°	
				80°						55°	
				−80°						−55°	
				−105°						−130°	

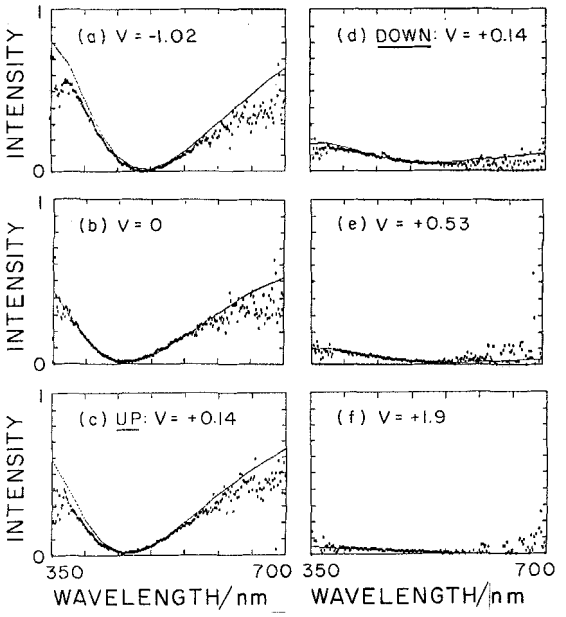

Figure 17. Change of transmission spectrum of a chevron cell with applied field. The sequence of normalized experimental spectra and model fits shown here are typical of those used to determine $\phi(x)$ in our chevron cell and correspond to the data in the first columns of tables 2 and 3. These are for $\alpha = +18°$ and a chevron interface 72% of the way from the botton of the cell. The other parameters are discussed in the text. The big change between (*c*) and (*d*) corresponds to the cell switching from UP to DOWN, the birefringence colour changing from yellow-pink to blue.

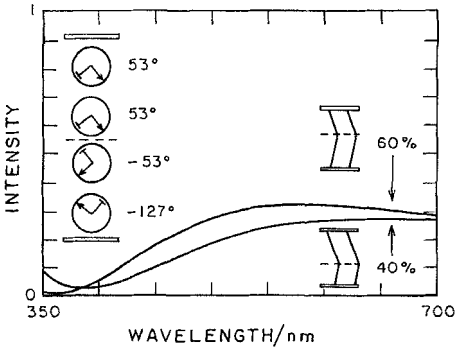

Figure 18. Change of transmission spectrum across a zig-zag defect. A model calculation shows that the main effect on the transmission spectrum of an asymmetrically-chevroned cell when the position of the chevron interface is reflected through the midplane of the cell is a change in the overall intensity, the colour remaining essentially the same. The model FLC is between crossed polarizers ($\Phi_P = 0°$, $\Phi_A = 90°$) at an orientation $\alpha = 0$ and the director structure is shown in the figure. Similar results are obtained for other values of α.

Table 3. Fitted director states in negative fields. This table shows the director structures of a chevron cell obtained by fitting measured transmission spectra at different negative voltages. The actual spectra for the first column are shown in figure 17. At each voltage we show the values of ϕ at the top of the cell, just above and just below the chevron interface, and at the bottom of the cell. '[poor]' indicates that the spectral fit was poor. Voltages in square brackets were the values used when the director field equation became insoluble using the actual experimental voltage.

Outside zig-zag loop (chevron at 72 per cent)						Inside zig-zag loop (chevron at 28 per cent)					
$\alpha = +18°$		$\alpha = -2°$		$\alpha = -22°$		$\alpha = +18°$		$\alpha = -2°$		$\alpha = -22°$	
N28	+0·14 V	N16	+0·53 V								
45°		53°									
118°		127°									
−118°		−127°									
−118°		−127°									
N27	0 V	N19	0 V			N13	−0·03 V				
50°		75°				70°	[poor]				
135°		130°				95°					
−135°		−130°				−95°					
−135°		−130°				−95°					
				N22	−0·41 V	N12	−0·66 V	N5	−0·51 V	N11	−0·68 V
				88°		75°	[poor]	86°	[−0·7]	100°	
				105°		97°		135°		120°	
				−105°		−97°		−135°		−120°	
				−105°		−97°		−135°		−120°	
N26	−102 V	N20	−1 V	N21	−1 V			N4	−1·69 V		
90°		102°	[−0·06]	105°	[−1·26]			105°			
150°		145°		135°				145°			
−150°		−145°		−135°				−145°			
−150°		−145°		−135°				−145°			
								N6	−10 V		
								120°			
								167°			
								−167°			
								−167°			

the cell from UP to DOWN. The spectra correspond to the data shown in the first columns of tables 2 and 3.

Finally, in support of our assertion that the intensity difference across a zig-zag line is due to reflection of the chevron interface through the mid-plane of the cell, we show in figure 18 two model spectra calculated for an idealized chevron cell in the DOWN state, oriented at $\alpha = 0$ between crossed polarizers. The spectra for the chevron at 40 and 60 per cent are seen to differ mainly in intensity and not in their overall shape. The short wavelengths, where they are most different, are outside the visible range of about 400–750 nm. The spectra for other orientations of the cell show similar behaviour. This intensity difference will be the topic of a subsequent publication [33].

6. Discussion

Our general level of success in fitting the spectral data presented in the previous section broadly confirms the validity of our model of director orientation in splayed chevron SSFLC cells. Before the true layer structure of chevron cells became known, we tried to model these cells using a single slab of uniformly tilted layers, but the calculated retardance of the model cell always changed far more with field than the measures spectra would allow, making it appear as though the cell thickness itself were changing with field. Including the chevron has eliminated this problem.

The few discrepancies in the fits are presumed to results more from inaccuracies in the physical parameters than from any fundamental flaw in the model itself. In future experiments it would help to know the true values of P/K and $\Delta n(\lambda)$. In addition, the layer tilt δ could be determined by performing an X-ray experiment on the same cell and the cell thickness found by some independent means (such as by optical interference in an air bubble). Cooling the scanner would help to reduce the background noise, thus producing clean spectra.

We conclude with a few comments on the general appropriateness of our model structures to real splayed chevron SSFLC cells. Our current 'best guess' at the director structure in chevron cells comes from solving a dynamical equation of motion, explicity including surface interactions at the chevron interface and the cell walls of the kind shown in equation (1) [12]. For calculating transmission spectra we have so far opted for the simpler approach of assuming that we have two somewhat independent FLC slabs with fixed (but adjustable) boundaries. In contrast with the full dynamical equation of motion, which is a non-linear partial differential equation, our Euler–Lagrange equation (equation (3)) is an ordinary differential equation that can largely by solved analytically. The final solution $\phi(x)$ can consequently be calculated very fast, even on a personal computer. This is an advantage because the same computer can be dedicated to gathering and displaying experimental data.

Ultimately, though, in order to measure the strengths of the surface anisotropies included in the fully dynamic model, one would really need to calculate director structures from this model too. Spectral fits would then be obtained by varying the surface energies directly, which in turn would automatically adjust the boundary angles. Solving the dynamic equation also allows the inclusion of such effects as the dielectric torques and electrostatic interactions caused by the self-interaction of the ferroelectric dipoles in each other's fields [34]. This last effect, which is expected to be important in FLC materials with high polarization, results in general in a spatially non-uniform electric field and different electrooptical properties.

7. Summary

In this paper, we have presented a model of director structure in splayed SSFLC chevron cells as a function of applied electric field. The model is based on an equilibrium zero-field structure that has the directors both at the boundaries and at the internal chevron interface oriented approximately parallel to the glass plates bounding the cell. By solving the appropriate differential equation of structure above and below the chevron, assuming fixed boundaries, we can find the variation of the director orientation in space as a function of applied field. The boundary angles can be varied to simulate the effects of the surface interaction energies.

Studies of the transmitted polarization state of light propagated through typical chevron structures indicate that the Mauguin limit is rarely obeyed in thin cells and then only at the very shortest optical wavelengths. Calculations of the visible transmission spectrum of such model structures have been compared with those obtained from real SSFLC cells. Preliminary results are very encouraging, confirming that the basic features of our model are correct. This technique promises to be a sensitive probe of the surface orientation in FLC cells but hysteresis effects and the limited amount of data available have thus far not allowed us to determine the nature of the cell surface anisotropies in any detail.

This work was supported by U.S. ARO and contract DAAL03-90-6-0002 and NSF/Engineering Research Center for Optoelectronic Computing Systems contract CDR 8622236.

References

[1] CLARK, N. A., and LAGERWALL, S. T., 1980, *Appl. Phys. Lett.*, **36**, 899.
[2] RIEKER, T. P., CLARK, N. A., SMITH, G. S., PARMAR, D. S., SIROTA, E. B., and SAFINYA, C. R., 1987, *Phys. Rev. Lett.*, **59**, 2658.
[3] CLARK, N. A., and RIEKER, T. P., 1988, *Phys. Rev.* A **37**, 1053.
[4] HANDSCHY, M. A., and CLARK, N. A., 1984, *Ferroelectrics*, **59**, 69.
[5] CLARK, N. A., and LAGERWALL, S. T., 1984, *Ferroelectrics*, **59**, 25.
[6] LEJECK, L., GLOGAROVA, M., and PAVEL, J., 1984, *Phys. Stat. Sol.* (*a*), **82**, 47. ISHIDAWA, K., UEMURA, T., TAKEZOE, H., and FUKUDA, A., 1987, *J. appl. Phys.*, **24**, L230.
[7] MACLENNAN, J. E., and CLARK, N. A., 1987, *International Conference on Raman and Luminescence Spectroscopy in Technology*, edited by J. E. Griffiths and F. Adar, *Proc. SPIE*, **822**, 47.
[8] TAKEZOE, H., OUCHI, Y., ISHIKAWA, K., and FUKUDA, A., 1986, *Molec. Crystals liq. Crystals*, **139**, 27.
[9] OUCHI, Y., TAKEZOE, H., and FUKUDA, A., 1987, *Jap. J. appl. Phys.*, **26**, 1.
[10] SHINGU, T., TSUCHIYA, T., OUCHI, Y., TAKEZOE, H., and FUKUDA, A., 1986, *Jap. J. appl. Phys.*, **25**, L206.
[11] AMAYA, P. G., HANDSCHY, M. A., and CLARK, N. A., 1984, *Opt. Engng.*, **23**, 261.
[12] MACLENNAN, J. E., CLARK, N. A., and HANDSCHY, M. A. (to be published).
[13] XUE, J.-Z., CLARK, N. A., and MEADOWS, M. R., 1988, *Appl. Phys. Lett.*, **53**, 2397.
[14] HIJI, N., OUCHI, Y., TAKEZOE, H., and FUKUDA, A., 1988, *J. appl. Phys.*, **27**, 8; 1988, *Ibid.*, **27**, L1.
[15] HANDSCHY, M. A., CLARK, N. A., and LAGERWALL, S. T., 1983, *Phys. Rev. Lett.*, **51**, 471.
[16] MACLENNAN, J. E., HANDSCHY, M. A., and CLARK, N. A., 1986, *Phys. Rev.*, A **34**, 3554.
[17] ABRAHAMOWITZ, M., and STEGUN, I. A., 1972, *Handbook of Mathematical Functions*, 9th edition (Dover).
[18] LOCKHART, T. E., ALLENDER, D. W., GELERINTER, E., and JOHNSON, D. L., 1979, *Phys. Rev.* A, **20**, 1655.
[19] ONG, H. L., and MEYER, R. B., 1983, *J. opt. Soc. Am.*, **73**, 167.
[20] BERREMAN, D. W., 1973, *J. opt. Soc. Am.*, **62**, 502; 1973, *Ibid.*, **63**, 1374.

[21] GAROFF, S., MEYER, R. B., and BARAKAT, R., 1978, *J. opt. Soc. Am.*, **68**, 1217.
[22] CHANDRASEKHAR, S., and SHASHIDHARA PRASAD, J., 1971, *Molec. Crystals liq. Crystals*, **14**, 115.
[23] Spectron Instrument Corp. (personal communication).
[24] HARK, S. K., HULL, V. J., and WYSOCKI, J. J. (preprint).
[25] WU, SHIN-TSON, 1986, *Phys. Rev.* A, **33**, 1270.
[26] CLARK, N. A., HANDSCHY, M. A., and LAGERWALL, S. T., 1983, *Molec Crystals liq. Crystals*, **94**, 213.
[27] W7 and W82 (which are 4′-c(s)-2-ethoxypropoxy-phenyl 4-(*n*-decyloxy) benzoate and 4′-c(s)-4-methylhexyloxy-phenyl 4-(*n*-decyloxy) benzoate respectively) are available from Displaytech Inc., 2200 Central Avenue, Boulder, Colorado 80301, U.S.A.
[28] CLARK, N. A., REIKER, T. P., and MACLENNAN, J. E., 1988, *Ferroelectrics*, **85**, 79.
[29] OUCHI, Y., TAKEZOE, H., and FUKUDA, A., 1988, *Ferroelectrics*, **85**, 113.
[30] BORN, M., and WOLF, E., 1980, *Principles of Optics*, 6th edition (Pergamon).
[31] CHANDRASEKHAR, S., 1977, *Liquid Crystals* (Cambridge University Press), p. 195.
[32] DE GENNES, P. G., 1974, *The Physics of Liquid Crystals* (Oxford University Press), p. 232.
[33] ZHIMING, Z., CLARK, N. A., MACLENNAN, J. E. (to be published).
[34] ZHIMING, Z., MACLENNAN, J. E., and CLARK, N. A., 1989, *Liquid Crystal Chemistry, Physics, and Applications*, edited by J. William Doane and Zui Yaniv; 1989. *Prov. S.P.I.E.*, **1080**, 110. PAUWELS, H., DEMAY, G., REYNAERTS, C., and CUYPERS, F., 1989, *Ferroelectrics*, **89**, 171.